J. Fluid Mech. (1969), *vol.* 36, *part* 4, *pp.* 759–783
Printed in Great Britain

Theory of transonic shear flow past a thin aerofoil

By MASANOBU NAMBA
Department of Aeronautical Engineering,
Kyushu University, Fukuoka, Japan

(Received 24 July 1968)

A generalized linear theory is developed for a compressible shear flow by extending the Fourier integral representations for the pressure field disturbed by pressure dipoles, and it is applied to a transonic shear flow past a thin aerofoil.

A method of determining the pressure distribution on the aerofoil surface is shown. Some numerical examples are presented and discussed.

It is found that the three-dimensional effect due to non-uniformity of the Mach number appears in the greatest degree at lower supersonic span-stations. Even within the scope of the linearized theory not such a great lift force arises near the sonic station as would be expected from the linearized uniform flow theory.

1. Introduction

As is well known, the two-dimensional cascade generally shows a great increase of pressure loss at transonic Mach numbers due to the occurrence of shock waves. This information had been enough for us to regard the transonic axial compressor as unpromising and to direct our attention towards the supersonic axial compressor in order to meet the requirement of high thrust/weight ratio for jet engines. However, experimental studies on actual axial compressors (Lieblein, Lewis & Sandercock 1952) revealed that they operate in contrast to expectation with relatively high efficiency throughout the transonic régimes. Consequently the transonic compressor has become of considerable interest to engine designers.

Such a difference in performance between the two-dimensional cascade and the actual compressor blade row seems to originate in the difference of the compressibility effect. When we think of the compressibility effect, it should be much emphasized that in the compressor blade row the resultant Mach number varies along the blade span. This seems an important factor that makes the transonic axial compressor operate relatively efficiently. The author and his colleague's (1965) experimental study on a linear cascade in transonic shear flows gives some evidence to support this view.

We have as yet little analytical information concerned with the compressibility effect in a transonic compressor except that by McCune (1958). His work, however, is confined to the non-lifting problem, i.e. the thickness problem, which seems of less interest to engine designers than the lifting problem. The latter problem is in general much more difficult to deal with than the former because we must evaluate the non-uniform downwash induced by the trailing vorticity. It should also be noted that the interference between blades as well as the transonic resonance make McCune's results too complicated to deduce the essential feature in the compressibility effect originating from the non-uniform Mach number itself.

In order to elucidate this essential feature, this paper treats a more simplified flow model like that adopted in the earlier papers (Namba & Asanuma 1967 and Namba 1969, to be referred to hereafter as L and S respectively), that is to say, a parallel shear flow passing through obstacles spanning two parallel walls. In this paper the problem is simplified further by dealing with a single thin aerofoil instead of a cascade.

In general the linearized theory cannot be applied to a steady uniform transonic flow. As pointed out by McCune (1958), this is due to the fact that the linearized theory assumes a disturbance to propagate relative to the undisturbed fluid at a sound speed appropriate to the undisturbed flow condition. This assumption makes disturbances accumulate in the case that the Mach number of the undisturbed flow is everywhere one and then the linear theory becomes physically meaningless. Therefore in this case we must take into account a non-linear term which ensures that disturbances propagate at the local speed of sound relative to the local fluid velocities.

In the case of a shear flow, however, the linearized theory is applicable even to a transonic régime, because the accumulation of disturbances is relieved owing to the non-uniform Mach number of the undisturbed condition. In this paper a linearized three-dimensional theory is developed by assuming small disturbances. In view of the author's (1965) experimental results the assumption of small disturbances is expected to be of practical validity for transonic shear flows as far as thin obstacles are concerned.

The fundamental differential equation for a transonic shear flow belongs to the mixed type which is elliptic in the subsonic region and hyperbolic in the supersonic region. Although the flow characters in both regions are essentially different from each other, no discontinuity in pressure and velocities should arise across the sonic plane. Therefore it is desirable to express them in common forms throughout both regions. For this purpose we shall, in this paper, generalize the Fourier integral representation of disturbance pressure due to pressure dipoles which has been derived for subsonic shear flow in L and S. Then, it is shown how to determine the surface pressure on a given aerofoil in a transonic shear flow. Finally, a few numerical examples are given and discussed.

2. Assumptions and basic equations

As shown in figure 1 we shall treat a thin aerofoil spanning two parallel walls denoted by $y = 0$ and $y = \lambda$. The aerofoil with the chord length of 1 is placed along the y-axis and attacked by a spanwisely non-uniform shear flow. For this flow model the following assumptions are made: (i) the fluid is an inviscid, non-conducting perfect gas; (ii) the aerofoil has small thickness and camber, and is located with a small angle of attack; (iii) the flow is a small-disturbance flow, and the entropy remains constant along each streamline; (iv) the Mach number gradient near the sonic station is not small.

The Mach number distribution along the y-axis is determined by

$$M_{-\infty}(y) = U(y)/\{\kappa p_{-\infty}/\rho_{-\infty}(y)\}^{\frac{1}{2}}, \tag{1}$$

where $U(y)$, $\rho_{-\infty}(y)$ and $p_{-\infty}$ are the velocity, the fluid density and the static pressure of the undisturbed stream respectively and κ denotes the ratio of the specific heats of the fluid.

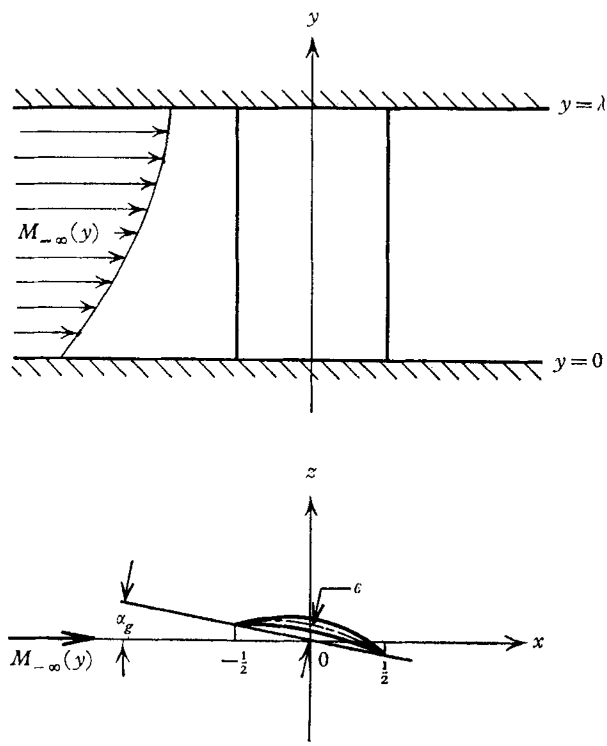

FIGURE 1. Geometry and notation of the flow model.

Since we deal with the transonic shear flow with a sonic flow velocity at a certain span-station, shock waves are expected to exist. However, we shall assume that the flow is disturbed so weakly that the entropy change across the shock waves can be neglected as a higher-order small perturbation. Then we find, as in L and S, a linearized equation for the disturbance pressure p as follows:

$$[1 - M^2_{-\infty}(y)]\frac{\partial^2 p}{\partial x^2} + \frac{\partial^2 p}{\partial y^2} + \frac{\partial^2 p}{\partial z^2} - \frac{2}{M_{-\infty}}\frac{dM_{-\infty}}{dy}\frac{\partial p}{\partial y} = 0. \tag{2}$$

Here a brief mention should be made of the validity of the linearization expressed by (2) in the transonic régime. It is certain that the first term on the left-hand side of (2) becomes small at a near-sonic flow station compared with neglected non-linear terms. However, according to Lighthill's (1950) investigation on two-dimensional shear flow, the disturbance in the sonic plane is found to be

$$\left.\begin{aligned} \partial p/\partial x &= O[(dM_{-\infty}/dy)^{-\frac{1}{6}}] \\ \partial p/\partial y &= O[(dM_{-\infty}/dy)^{\frac{5}{6}}] \end{aligned}\right\} \quad \text{at} \quad M_{-\infty} = 1.$$

Although this is a result for a two-dimensional flow field, it may be possible to say that, unless $dM_{-\infty}/dy$ is small near sonic stations, the non-linear terms with respect to $\partial p/\partial x$ still remain small in comparison with the retained linear terms other than the first one in (2).

The boundary condition to be fulfilled at the side walls is

$$\partial p/\partial y = 0 \quad \text{for} \quad y = 0, \lambda. \tag{3}$$

The linearized boundary condition on the aerofoil surface can be written as

$$[w/U]_{z=\pm 0} = f(x) \quad \text{for} \quad -\tfrac{1}{2} < x < \tfrac{1}{2}, \tag{4}$$

where w is the z-component of the disturbance velocity and $f(x)$ describes the slope of the aerofoil surface which is assumed for simplicity to be uniform along the span. Here we shall deal with the lifting problem only, and hence $f(x)$ denotes the slope of the aerofoil mean camber surface including the angle of attack. On the thickness problem some comments are given in appendix C.

In the case of a transonic shear flow non-zero disturbance is expected to exist upstream of the aerofoil even in the supersonic region where $M_{-\infty}(y) > 1$, because disturbance can propagate upstream by way of the subsonic region where $M_{-\infty}(y) < 1$. On the other hand the disturbance propagating downstream in the supersonic region can remain finite at infinity. Therefore the boundary condition at infinity is written as

$$p \to 0 \quad \text{as} \quad x \to -\infty \tag{5}$$

and

$$|p| < \infty \quad \text{for} \quad x \to +\infty. \tag{6}$$

It should be noted, however, that the expressions (5) and (6) hold also for a pure supersonic or a pure subsonic shear flow, since the solution for a pure supersonic shear flow satisfying the condition (5) automatically gives zero disturbance upstream of the aerofoil, while in the case of a pure subsonic shear flow the disturbance obtained from the solution satisfying the condition (6) necessarily vanishes far downstream.

3. General solution and its property

As shown in L and S, the solution of (2) satisfying (3) is in general expressed as follows:

$$p = \int_0^\infty \sum_{n=0}^{\infty} A_n(\alpha) \exp(i\alpha x + \beta_n(\alpha) z)\, Y_n(y;\alpha)\, d\alpha, \tag{7}$$

where $\beta_n(\alpha)$ and $Y_n(y;\alpha)$ $(n = 0, 1, 2, \ldots)$ are respectively the eigenvalues and the eigenfunctions for the following Sturm–Liouville boundary-value problem:

$$\frac{d}{dy}\left(\frac{1}{M^2_{-\infty}}\frac{dY}{dy}\right) + \left(-\frac{1-M^2_{-\infty}}{M^2_{-\infty}}\alpha^2 + \frac{1}{M^2_{-\infty}}\beta^2\right) Y = 0, \tag{8}$$

$$dY/dy = 0 \quad \text{at} \quad y = 0, \lambda. \tag{9}$$

Here $A_n(\alpha)$ is an arbitrary function of α which is to be determined by the other boundary conditions. The eigenfunctions $Y_n(y;\alpha)$ constitute a complete set of orthonormal functions such that

$$\frac{1}{\lambda}\int_0^\lambda \frac{Y_n Y_m}{M_{-\infty}^2}dy = \delta_{n,m}, \tag{10}$$

where $\delta_{n,m}$ is the Kronecker delta.

Now, let $Y_n(y;\alpha)$ be expressed in terms of a series such that

$$Y_n(y;\alpha) = \sum_{m=0}^{\infty} B_{n,m}(\alpha)\, Y_m(y;0). \tag{11}$$

Then, as shown in S, $\beta_n^2(\alpha)/\alpha^2$ $(n = 0, 1, 2, \ldots)$ are obtained as the eigenvalues of a certain infinite matrix, and $B_{n,m}(\alpha)$ $(m = 0, 1, 2, \ldots)$ are corresponding eigenvectors. It is shown from the property of the matrix that

$$\left.\begin{aligned} \beta_n^2(\alpha)/\alpha^2 &= q_n^2 + O(\alpha^{-2}),\\ B_{n,m}(\alpha) &= B_{n,m}(\infty) + O(\alpha^{-2}), \end{aligned}\right\} \quad \text{as} \quad \alpha \to \infty, \tag{12}$$

$$\left.\begin{aligned} \beta_n^2(\alpha)/\alpha^2 &= \begin{cases} 1 - \bar{M}_{-\infty}^{*2} + O(\alpha^2): n = 0,\\ O(\alpha^{-2}): n = 1, 2, \ldots, \end{cases}\\ B_{n,m}(\alpha) &\to \delta_{n,m}, \end{aligned}\right\} \quad \text{as} \quad \alpha \to 0, \tag{13}$$

where q_n and $B_{n,m}(\infty)$ are finite values and $\bar{M}_{-\infty}^*$ denotes the harmonic mean Mach number defined by

$$\bar{M}_{-\infty}^* \equiv \left(\frac{1}{\lambda}\int_0^\lambda \frac{1}{M_{-\infty}^2}dy\right)^{-\frac{1}{2}}. \tag{14}$$

As shown in L, in the case of a pure subsonic shear flow $\beta_n^2(\alpha)$ is always positive for $0 < \alpha < \infty$, and hence $0 < q_n^2$. In the case of a transonic shear flow, however, not all of β_n^2 remain positive as $\alpha \to \infty$. In fact, let the terms of order higher than $m = N$ in the series (11) be omitted, then $\beta_n^2(\alpha)/\alpha^2$ $(n = 0, 1, 2, \ldots, N-1)$ can be obtained as the eigenvalues of a finite matrix of order N. Then it turns out that there exist an integral number N' and real numbers α_n such that

$$\left.\begin{aligned} &\beta_n^2(\alpha)/\alpha^2 \begin{cases} > 0 & \text{for} \quad \alpha_n > \alpha > 0,\\ = 0 & \text{for} \quad \alpha = \alpha_n,\\ < 0 & \text{for} \quad \alpha > \alpha_n, \end{cases}\\ &\infty > \alpha_n > 0 \quad \text{for} \quad N' > n \geqslant 0, \quad \text{and} \quad \alpha_n = \infty \quad \text{for} \quad N-1 \geqslant n \geqslant N'. \end{aligned}\right\} \tag{15}$$

The number of the eigenvalues which become negative as $\alpha \to \infty$, i.e. N', increases with increase of the region of supersonic flow. According as the flow is entirely subsonic, transonic or entirely supersonic, there holds $N' = 0$, $N > N' \geqslant 1$ or $N' = N$. To demonstrate such a nature of $\beta_n(\alpha)$, three examples of the dependence of $\beta_n^2(\alpha)/\alpha^2$ upon α are shown for shear flows with the Mach number profile of $M_{-\infty}(y) = M_0 e^{ay/\lambda}$ in figures 2, 3 and 4, where N is chosen as 10 and M_1 denotes $M_{-\infty}(\lambda) = M_0 e^a$.

The negative value of $\beta_n^2(\alpha)$ implies that $\beta_n(\alpha)$ is purely imaginary. It is evident that the disturbance expressed in terms of purely imaginary values of $\beta_n(\alpha)$ in

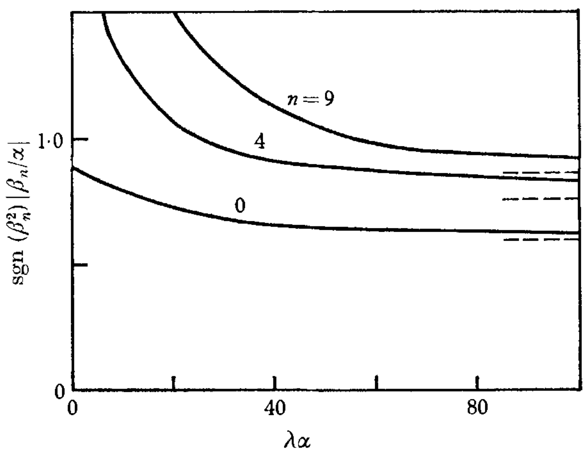

FIGURE 2. Dependence of the eigenvalues β_n upon the parameter α for a subsonic shear flow of $a = 1{\cdot}0$, $M_0 = 0{\cdot}3$ and $M_1 = 0{\cdot}815$. – – –, value for $\lambda\alpha = \infty$. ($N = 10$.)

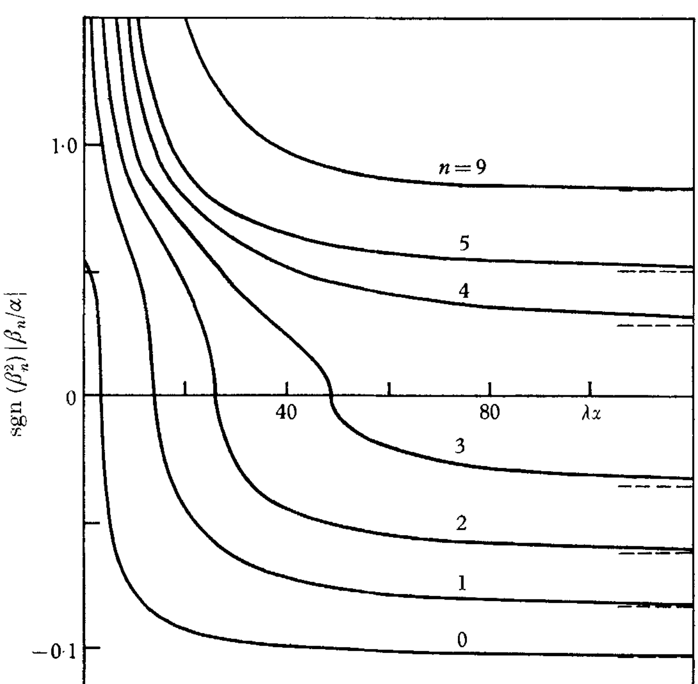

FIGURE 3. Dependence of the eigenvalues β_n upon the parameter α for a transonic shear flow of $a = 1{\cdot}0$, $M_0 = 0{\cdot}550$ and $M_1 = 1{\cdot}495$. – – –, value for $\lambda\alpha = \infty$. ($N = 10$.)

(7) is of supersonic character. The dependence of the character of disturbance upon whether $\beta_n(\alpha)$ is real or imaginary can be confirmed, if the expression (7) is applied to a uniform flow as a well-known extreme case. When the flow field is uniform in the spanwise direction, that is, when $M_{-\infty}(y) = M_0$ = constant and

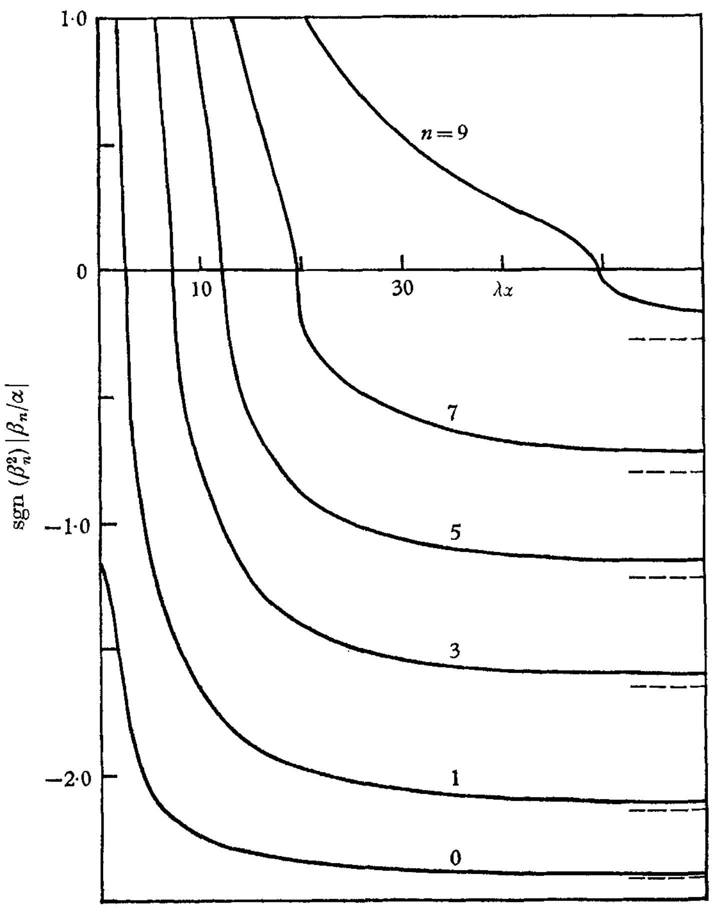

FIGURE 4. Dependence of the eigenvalues β_n upon the parameter α for a supersonic shear flow of a = 1·0, M_0 = 1·0 and M_1 = 2·718. – – –, value for $\lambda\alpha = \infty$. (N = 10.)

$\partial p/\partial y = 0$, the eigenvalue $\beta_0(\alpha)$ reduces to $\alpha\sqrt{(1-M_0^2)}$ and the solution corresponding to (7) becomes

$$p = \int_0^\infty A(\alpha)\exp(i\alpha x + \alpha\sqrt{(1-M_0^2)}z)\,d\alpha.$$

4. Disturbance pressure due to a lifting-surface

The pressure jump $\Delta p_s(x,y)$ across the aerofoil can be represented in terms of a series such that

$$\Delta p_s(x,y) \equiv [p]_{z=-0} - [p]_{z=+0} = 2\pi \sum_{n=0}^{\infty} F_n(x;\alpha)\, Y_n(y;\alpha). \tag{16}$$

From the orthogonality of $Y_n(y;\alpha)$ shown by (10), it follows that

$$F_n(x;\alpha) = \frac{1}{2\pi}\frac{1}{\lambda}\int_0^{\lambda} \frac{Y_n(y;\alpha)}{M_{-\infty}^2(y)} \Delta p_s(x,y)\, dy. \tag{17}$$

Now, the solution for a subsonic shear flow given in L and S suggests that the expression of disturbance pressure appropriate to the present problem may be given by

$$p = -\operatorname{sgn} z \int_{-\frac{1}{2}}^{\frac{1}{2}} d\xi \int_0^{\infty} \sum_{n=0}^{\infty} \mathscr{R}[\exp(i\alpha(x-\xi) - \beta_n(\alpha)|z|)]\, F_n(\xi;\alpha)\, Y_n(y;\alpha)\, d\alpha, \tag{18}$$

where $\mathscr{R}[\ ]$ denotes the real part, and the argument is assigned for $\beta_n(\alpha)$ as follows:

$$\left.\begin{aligned} \beta_n(\alpha) &= |\beta_n(\alpha)| \quad \text{for} \quad \alpha_n > \alpha > 0,\\ \beta_n(\alpha) &= i|\beta_n(\alpha)| \quad \text{for} \quad \alpha > \alpha_n. \end{aligned}\right\} \tag{19}$$

Such an appointment of the sign corresponds to the boundary condition at infinity which requires that the subsonic disturbance vanishes at infinity and that the supersonic disturbance propagates only in the downstream direction.

The proof that the representation (18) satisfies the boundary conditions (3), (5) and (6) is shown in appendix A.

It would be instructive to show that the expression (18) is a generalization which holds also for a subsonic shear flow or a two-dimensional flow. For a subsonic shear flow, since $\beta_n(\alpha)$ is always real,

$$\mathscr{R}[\exp(i\alpha(x-\xi) - \beta_n(\alpha)|z|)] = \cos\{\alpha(x-\xi)\}\exp(-\beta_n(\alpha)|z|).$$

Then it may not be difficult to show that (18) reduces to the expression given in S. In the case of a supersonic uniform flow, where $M_{-\infty}(y) = M_0 = \text{constant}$,

$$F_0(x;\alpha) = \Delta p_s(x)/2\pi,$$
$$F_n(x;\alpha) = 0 \quad \text{for} \quad n = 1, 2, \ldots,$$
$$\beta_0(\alpha) = i\alpha\sqrt{(M_0^2 - 1)}.$$

Then (18) degenerates to the following well-known relation:

$$\begin{aligned} p &= -\frac{\operatorname{sgn} z}{2\pi}\int_{-\frac{1}{2}}^{\frac{1}{2}} \Delta p_s(\xi)\, d\xi \int_0^{\infty} \cos\{\alpha[x-\xi-|z|\sqrt{(M_0^2-1)}]\}\, d\alpha \\ &= -\operatorname{sgn} z \frac{1}{2}\int_{-\frac{1}{2}}^{\frac{1}{2}} \Delta p_s(\xi)\, \delta(x-\xi-|z|\sqrt{(M_0^2-1)})\, d\xi \\ &= \begin{cases} -\frac{1}{2}\operatorname{sgn} z\, \Delta p_s(x-|z|\sqrt{(M_0^2-1)}) & \text{for} \quad \frac{1}{2} \geqslant |x-|z|\sqrt{(M_0^2-1)}|, \\ 0 & \text{for} \quad \frac{1}{2} < |x-|z|\sqrt{(M_0^2-1)}|. \end{cases} \end{aligned}$$

5. Upwash distribution

Our purpose is to determine the pressure distribution on the lifting-surface, i.e. $\Delta p_s(x,y)$, or in other words the coefficients $F_n(x;\alpha)$, for the given geometrical condition (4). Therefore it is necessary to derive the expression of the upwash on the lifting-surface, $[w/U]_{z=0}$. This is obtainable by integrating the z-component of the equation of motion as

$$\left[\frac{w}{U}\right]_{z=0} = \lim_{z\to 0}\left[-\frac{1}{\kappa p_{-\infty}M^2_{-\infty}}\int_{-\infty}^{x}\frac{\partial p}{\partial z}dx\right], \tag{20}$$

where the condition that the disturbance velocity vanishes at $x = -\infty$ is used.

Considering the relation

$$F_n(x;\alpha) = \sum_{m=0}^{\infty} B_{n,m}(\alpha)F_m(x;0) \tag{21}$$

which follows from (11) and (17), and omitting the terms of order greater than N in the infinite series, we get the upwash distribution in the following refined form:

$$\left[\frac{w}{U}\right]_{z=0} = -\frac{4\pi}{\kappa p_{-\infty}M^2_{-\infty}}\int_{-\frac{1}{2}}^{\frac{1}{2}}\sum_{n=0}^{N-1}F_n^{(0)}(\xi) \times\left[\tfrac{1}{8}\beta_n^{(0)}Y_n^{(0)}(y)+\sum_{m=0}^{N-1}D_{n,m}(x-\xi)\,Y_m^{(0)}(y)\right]d\xi, \tag{22}$$

where

$$\begin{aligned}D_{n,m}(x-\xi) = \frac{1}{4\pi}\sum_{k=0}^{N-1}\Bigg[&\int_0^{\alpha_k}\sin\{\alpha(x-\xi)\}\frac{\beta_k(\alpha)}{\alpha}B_{k,n}(\alpha)B_{k,m}(\alpha)\,d\alpha\\ &+\int_{\alpha_k}^{\infty}\cos\{\alpha(x-\xi)\}\left\{\frac{|\beta_k(\alpha)|}{\alpha}B_{k,n}(\alpha)B_{k,m}(\alpha)-|q_k|B_{k,n}(\infty)B_{k,m}(\infty)\right\}d\alpha\\ &+\left\{\pi\delta(x-\xi)-\frac{\sin\alpha_k(x-\xi)}{x-\xi}\right\}|q_k|\,B_{k,n}(\infty)B_{k,m}(\infty)\Bigg]\\ &+\frac{1}{4\pi}\sum_{k=N'}^{N-1}\Bigg[\int_0^{\infty}\sin\{\alpha(x-\xi)\}\left\{\frac{\beta_k(\alpha)}{\alpha}B_{k,n}(\alpha)B_{k,m}(\alpha)\right.\\ &\left.-|q_k|B_{k,n}(\infty)B_{k,m}(\infty)\right\}d\alpha+\frac{1}{x-\xi}|q_k|B_{k,n}(\infty)B_{k,m}(\infty)\Bigg]\end{aligned} \tag{23}$$

and $$\beta_n^{(0)} \equiv \beta_n(0),\quad Y_n^{(0)}(y) \equiv Y_n(y;0),\quad F_n^{(0)}(x) \equiv F_n(x;0). \tag{24}$$

A detailed description of deriving (22) will be found in appendix B. Note that $D_{n,m}(x-\xi)$ includes two singularities. One is of supersonic character denoted by $\delta(x-\xi)$, and the other is of subsonic character manifested by $1/(x-\xi)$. According as the basic flow is entirely subsonic ($N' = 0$) or entirely supersonic ($N' = N$), the term $\delta(x-\xi)$ or $1/(x-\xi)$ vanishes. For a transonic shear flow ($0 < N' < N$), both singularities are retained.

6. Integral equations and method of solution

Combination of (22) with (4) gives

$$-\frac{4\pi}{\kappa p_{-\infty} M_{-\infty}^2}\int_{-\frac{1}{2}}^{\frac{1}{2}} \sum_{n=0}^{N-1} F_n^{(0)}(\xi)\left[\tfrac{1}{8}\beta_n^{(0)} Y_n^{(0)}(y) + \sum_{m=0}^{N-1} D_{n,m}(x-\xi)\, Y_m^{(0)}(y)\right] d\xi = f(x) \quad (25)$$

for $-\frac{1}{2} < x < \frac{1}{2}$. Multiplying (25) by $Y_m^{(0)}(y)$ and integrating with respect to y from 0 to λ, we get the following simultaneous integral equations:

$$-\frac{4\pi}{\kappa p_{-\infty}}\int_{-\frac{1}{2}}^{\frac{1}{2}} \sum_{n=0}^{\infty} F_n^{(0)}(\xi)\,[\tfrac{1}{8}\beta_m^{(0)}\delta_{n,m} + D_{n,m}(x-\xi)]\, d\xi = \overline{Y}_m^{(0)} f(x)$$

$$(-\tfrac{1}{2} < x < \tfrac{1}{2},\ m = 0, 1, 2, \ldots, N-1), \quad (26)$$

where
$$\overline{Y}_m^{(0)} = \frac{1}{\lambda}\int_0^{\lambda} Y_m^{(0)}(y)\, dy. \quad (27)$$

Introducing the angle variables θ and ϕ defined as

$$x = \tfrac{1}{2}\cos\theta, \quad \xi = \tfrac{1}{2}\cos\phi \quad (0 < \theta, \phi < \pi), \quad (28)$$

we can rewrite (26) as

$$-\frac{4\pi}{\kappa p_{-\infty}}\int_0^{\pi} \sum_{n=0}^{N-1} F_n^{(0)*}(\phi)\,[\tfrac{1}{8}\beta_n^{(0)}\delta_{n,m} + D_{n,m}^*(\theta,\phi)]\,\tfrac{1}{2}\sin\phi\, d\phi = \overline{Y}_m^{(0)} f^*(\theta)$$

$$(0 < \theta < \pi,\ m = 0, 1, 2, \ldots, N-1), \quad (26a)$$

where
$$\left.\begin{aligned} &F_n^{(0)*}(\theta) \equiv F_n^{(0)}(\tfrac{1}{2}\cos\theta), \quad f^*(\theta) \equiv f(\tfrac{1}{2}\cos\theta), \\ &D_{n,m}^*(\theta,\phi) = D_{n,m}(\tfrac{1}{2}\cos\theta - \tfrac{1}{2}\cos\phi). \end{aligned}\right\} \quad (29)$$

In the case of a pure subsonic shear flow as shown in S, it is quite useful to represent $F_n^{(0)*}(\phi)$ in terms of a trigonometric series including $\tan\frac{1}{2}\phi$ which suitably expresses the square root singularity at the leading edge as well as the zero pressure jump (i.e. the Kutta's condition) at the trailing edge. However, in the case of a transonic or a supersonic shear flow, such a representation seems inappropriate, because in a supersonic region the pressure jump across the aerofoil surface at both of the leading and trailing edges can remain finite. Therefore it should be unreasonable to presume the pressure jump to be zero at the trailing edge and infinite at the leading edge in a transonic shear flow.

If we assume Δp_s at the trailing edge to be finite, instead of assuming it to be zero, then what will follow from it? Owing to the subsonic singularity $1/(x-\xi)$ included in the kernel function $D_{n,m}(x-\xi)$, $F_n^{(0)}(x)$ should generally involve a term $A/(\frac{1}{2}-x)^{\frac{1}{2}}$, where A is an arbitrary constant. It will be noted, therefore, that the condition mentioned above requires A to be zero, since otherwise Δp_s becomes infinite in order of $(\frac{1}{2}-x)^{-\frac{1}{2}}$ as $x \to \frac{1}{2}$. Therefore we can express the condition that Δp_s is bounded at $x = \frac{1}{2}$ in the form

$$\Delta p_s (\tfrac{1}{2}-x)^{\frac{1}{2}} = 0 \quad \text{at} \quad x = \tfrac{1}{2}. \quad (30)$$

It must be noted further that, in the case of a pure subsonic flow, the condition (30) automatically yields

$$\Delta p_s = 0 \quad \text{at} \quad x = \tfrac{1}{2}$$

as long as $f(x)$ is bounded at $x = \frac{1}{2}$.

In this view, let us introduce new unknown variables $\Phi_n^*(\phi)$ or $\Phi_n(\xi)$ defined by

$$\left.\begin{aligned}\Phi_n^*(\phi) &= F_n^{(0)*}(\phi)\,\tfrac{1}{2}\sin\phi,\\ \Phi_n(\xi) &= F_n^{(0)}(\xi)\,(\tfrac{1}{4}-\xi^2)^{\frac{1}{2}},\end{aligned}\right\} \tag{31}$$

then (26*a*) is rewritten as

$$-\frac{4\pi}{\kappa p_{-\infty}}\int_0^\pi \sum_{n=0}^{N-1}\Phi_n^*(\phi)\,[\tfrac{1}{8}\beta_n^{(0)}\delta_{n,m}+D_{n,m}^*(\theta,\phi)]\,d\phi = \overline{Y}_m^{(0)}f^*(\theta)$$
$$(m = 0,1,2,\ldots,N-1), \tag{32}$$

and we can give as the condition at the trailing edge

$$\Phi_n^*(0) = 0. \tag{33}$$

It should be noticed that for a flat plate in a uniform subsonic flow $\Delta p_s(\frac{1}{4}-x^2)^{\frac{1}{2}}$ shows a linear variation proportional to $\frac{1}{2}-x$, while in a uniform supersonic flow it shows a half-circle distribution proportional to $(\frac{1}{4}-x^2)^{\frac{1}{2}}$.

Since $\Phi_n^*(\phi)$ given by (31) are considered to be bounded for $0 < \phi < \pi$, a method of numerical integration with respect to ϕ is expected to give a solution of (32) with satisfactory accuracy. Therefore, if we take $M+1$ representative abscissae ϕ_i $(i = 0,1,2,\ldots,M)$ in $0 \leqslant \phi_i \leqslant \pi$ and choose ϕ_M as $\phi_M = 0$, then we get from (32) and (33) the following simultaneous linear equations for $N \times M$ unknowns $\Phi_n^*(\phi_i)$:

$$-\frac{4\pi}{\kappa p_{-\infty}}\sum_{i=0}^{M-1}\sum_{n=0}^{N-1}\Phi_n^*(\phi_i)\,[\tfrac{1}{8}\beta_n^{(0)}\delta_{n,m}+D_{n,m}^*(\theta_k,\phi_i)]\,w_i = \overline{Y}_m^{(0)}f^*(\theta_k)$$
$$(m = 0,1,2,\ldots,N-1,\; k = 0,1,2,\ldots,M-1), \tag{34}$$

where w_i denote weights which depend upon the adopted formula of the numerical quadrature.

7. Several aerodynamic characteristics

Once $\Phi_n(x)$ and hence $F_n^{(0)}(x)$ are determined, we can calculate various aerodynamic characteristics from them. In the following are shown the expressions for some of those considered to be of importance.

Local pressure jump coefficient across the aerofoil:

$$\begin{aligned}C_p &\equiv \Delta p_s(x,y)/\{\tfrac{1}{2}\kappa p_{-\infty}M_{-\infty}^2(y)\}\\ &= 4\pi\sum_{n=0}^{N-1}F_n^{(0)}(x)\,Y_n^{(0)}(y)/\{\kappa p_{-\infty}M_{-\infty}^2(y)\}.\end{aligned} \tag{35}$$

Local lift force per unit span:

$$\begin{aligned}l(y) &\equiv \int_{-\frac{1}{2}}^{\frac{1}{2}}\Delta p_s(x,y)\,dx\\ &= 2\pi\sum_{n=0}^{N-1}\overline{F}_n^{(0)}\,Y_n^{(0)}(y),\end{aligned} \tag{36}$$

where

$$\overline{F}_n^{(0)} \equiv \int_{-\frac{1}{2}}^{\frac{1}{2}}F_n^{(0)}(x)\,dx. \tag{37}$$

Local lift coefficient: $C_l(y) \equiv l(y)/\{\frac{1}{2}\kappa p_{-\infty} M^2_{-\infty}(y)\}$. (38)

Induced velocities on the wake surface far downstream:

$$\left[\frac{v_\infty}{U}\right]_{z=\pm 0} = \pm \frac{\pi}{\kappa p_{-\infty} M^2_{-\infty}} \sum_{n=1}^{N-1} \bar{F}^{(0)}_n \frac{dY^{(0)}_n}{dy}, \tag{39}$$

$$\left[\frac{w_\infty}{U}\right]_{z=0} = -\frac{\pi}{\kappa p_{-\infty} M^2_{-\infty}} \sum_{n=1}^{N-1} \bar{F}^{(0)}_n \beta^{(0)}_n Y^{(0)}_n(y), \tag{40}$$

where v_∞ and w_∞ are the y- and z-components of the induced velocity far downstream respectively.

Let us introduce an 'absolute lift coefficient' defined by

$$C^*_l(y) \equiv l(y)/\{\tfrac{1}{2}\kappa p_{-\infty} \bar{M}^{*2}_{-\infty}\}; \tag{41}$$

then $C^*_l(y)$ shows a spanwise distribution which is proportional to the local lift force $l(y)$.

8. Numerical examples and discussion

8.1. *Flow model and conditions in computation*

As in L and S, the Mach number profile of exponential variation is adopted in the present paper too, that is

$$M_{-\infty}(y) = M_0 \exp(ay/\lambda).$$

The expressions for $Y^{(0)}_n(y)$ and $\beta^{(0)}_n$ for this flow will be found in L and S. In order to make clear the effect of compressibility the results for four different Mach number levels with the same shear parameter $a = 1{\cdot}0$ are shown here.

The aerofoil configuration chosen is a flat plate with aspect ratio of $\lambda = 2{\cdot}5$.

The trapezoidal rule formula is applied to the numerical integration in (34); i.e. the arguments ϕ_i and the weights w_i are

$$\phi_i = \tfrac{1}{2}\pi + (i/M)\pi \quad \text{for} \quad i = 0, 1, 2, \ldots, M,$$

$$w_i = \begin{cases} \pi/M & \text{for} \quad i = 1, 2, \ldots, M-1, \\ \pi/(2M) & \text{for} \quad i = 0, M. \end{cases}$$

On the other hand the arguments θ_k at which (34) is to be satisfied are set at the middle station between the adjacent two abscissae ϕ_k and ϕ_{k+1}, i.e.

$$\theta_k = \phi_k + \pi/(2M) \quad (k = 0, 1, 2, \ldots, M-1).$$

Both of the numbers N and M are chosen to be 10.

The numerical integration of the Fourier integrals included in $D_{n,m}(x-\xi)$ has been performed by the same method as that adopted in the reference S. Since the number of unknowns to be determined by solving a set of linear equations is 100 in this case, the numerical work consumes much more time than in the case of the reference S. Furthermore, it has turned out that both of the numbers N and M greater than 10 would be desirable in order to evaluate the pressure and velocity distributions with a practically sufficient accuracy, since in the case of a transonic shear flow the spanwise and chordwise variations of the pressure and velocities near sonic flow stations are found to be complicated and hence the convergence of the series expansions such as (16) may not be rapid. Therefore some of the numerical results presented here may give no more than qualitative information as to the distribution patterns of pressure or velocities.

The computation was conducted on the electronic computer HITAC 5020E at the Computing Center of the University of Tokyo. The time consumed in computational work per case was about 700 seconds.

8.2. *The results*

Pressure distribution on a flat plate. The distributions of the pressure jump coefficient C_p/α_g are shown in figures 5–8, where the distributions of $C_p(\frac{1}{4}-x^2)^{\frac{1}{2}}/\alpha_g$ are also illustrated. Here α_g denotes the angle of attack.

For an entirely subsonic shear flow (figure 5) the chordwise variation of C_p is essentially similar in character to that in a uniform subsonic flow. As is confirmed already in the previous paper S, no singular phenomenon is seen near the sonic span-stations even within the scope of linear theory.

Figures 6 and 7 show the examples for transonic shear flows. It is interesting that the chordwise pressure profile keeps the uniform subsonic type of character over the whole subsonic span portion where $M_{-\infty} < 1$, while C_p at the lower supersonic span-station shows a complicated wavy profile. The chordwise variation of C_p seems most violent at the sonic span-station and it gradually diminishes as the distance from the sonic span-station increases. It is worth noticing that no pressure discontinuity across the lifting-surface is seen at the trailing edge, as long as the span-station belongs to the subsonic region, while at the span-station attacked by supersonic Mach number the pressure at the trailing edge shows a finite discontinuity across the aerofoil surface.

It appears that the pressure becomes infinite at the leading edge even in the supersonic region, since in strictness $C_p(\frac{1}{4}-x^2)^{\frac{1}{2}}$ must be zero at $x = -\frac{1}{2}$, in order for C_p to be finite at the leading edge. However, that the numerically obtained value of $C_p(\frac{1}{4}-x^2)^{\frac{1}{2}}$ is not precisely zero at $x = -\frac{1}{2}$ in the supersonic region may also be considered to originate from the inaccuracy in the numerical computation especially due to insufficient convergence of the adopted truncated series expansion. On the other hand if we judge from extrapolation of the values near $x = -\frac{1}{2}$, it also seems possible to regard the pressure at the leading edge as finite, which may be more reasonable from a theoretical point of view.

Figure 8 is the case where the whole span is attacked by a supersonic flow. The waviness of the C_p profile diminishes as $M_{-\infty}$ increases and completely vanishes at higher supersonic span-stations, where C_p shows a flat distribution similar in character to that of a flat plate in a uniform supersonic flow.

All the results indicate that the surface pressure at the lower supersonic span-station shows both the subsonic and supersonic characters in its pattern, the latter of which becomes dominant as $M_{-\infty}$ increases. On the other hand little of the supersonic character seems to be contained at high subsonic span-stations. One of the reasons for this phenomenon may be that disturbances transmitted across the sonic plane into the subsonic flow region propagate in all directions,

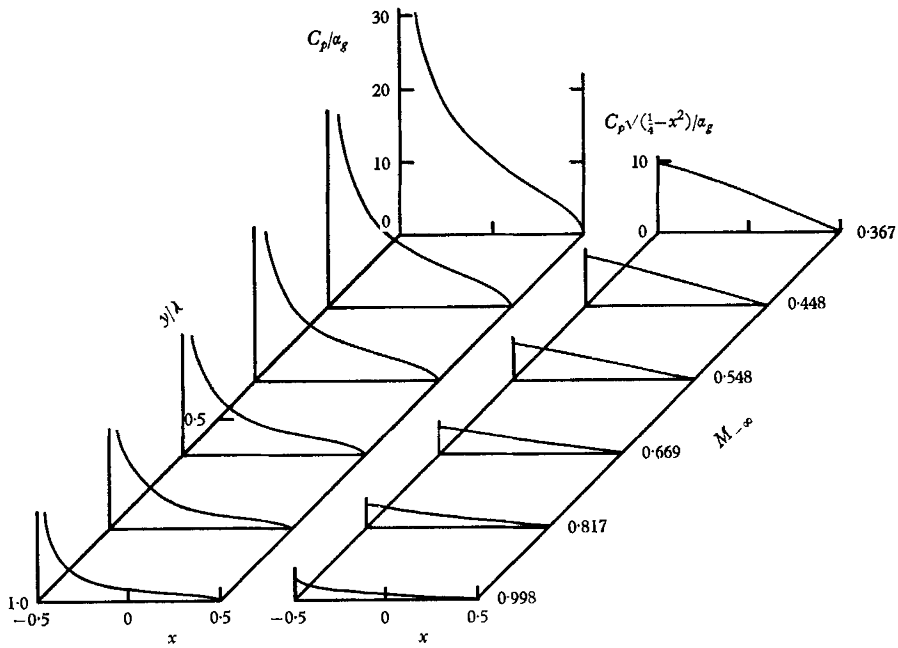

FIGURE 5. Distribution of the pressure coefficient for a flat plate of $\lambda = 2{\cdot}5$ in a subsonic shear flow of $a = 1{\cdot}0$, $M_0 = 0{\cdot}367$ and $M_1 = 0{\cdot}998$.

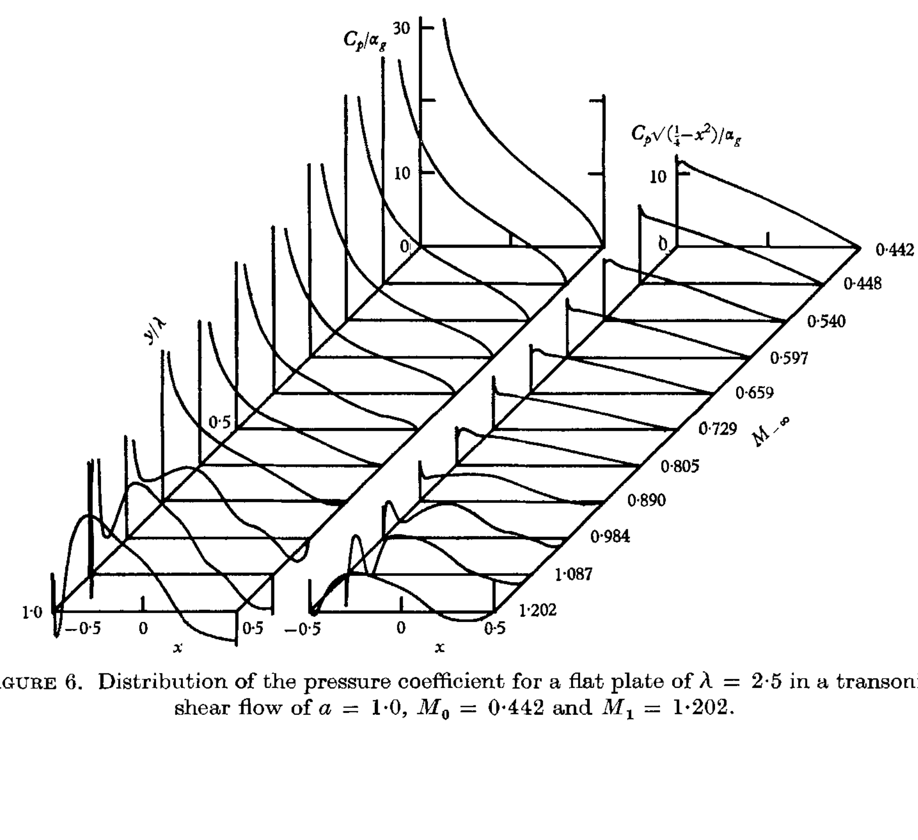

FIGURE 6. Distribution of the pressure coefficient for a flat plate of $\lambda = 2{\cdot}5$ in a transonic shear flow of $a = 1{\cdot}0$, $M_0 = 0{\cdot}442$ and $M_1 = 1{\cdot}202$.

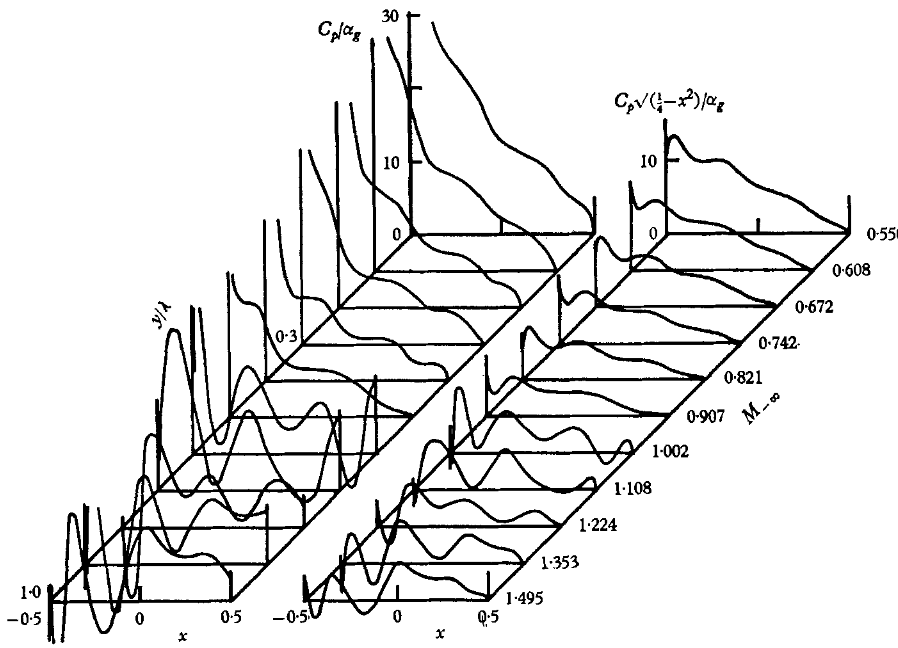

FIGURE 7. Distribution of the pressure coefficient for a flat plate of $\lambda = 2{\cdot}5$ in a transonic shear flow of $a = 1{\cdot}0$, $M_0 = 0{\cdot}550$ and $M_1 = 1{\cdot}495$.

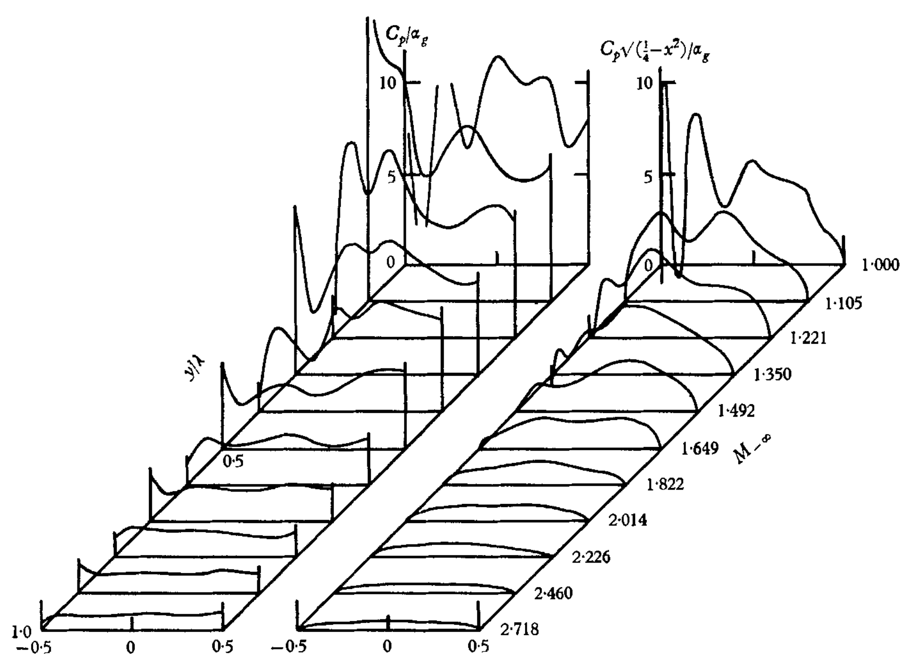

FIGURE 8. Distribution of the pressure coefficient for a flat plate of $\lambda = 2{\cdot}5$ in a supersonic shear flow of $a = 1{\cdot}0$, $M_0 = 1{\cdot}0$ and $M_1 = 2{\cdot}718$.

being smoothed out through a shorter distance. On the other hand, once the disturbance pressure originating from the subsonic flow region crosses the sonic plane into the supersonic flow region, then it can propagate only downstream in the local Mach conoid and thus decays only gradually.

Since there remains a little doubt on the degree of accuracy in the numerical computation, it would be too hasty to conclude that the obtained complicated wavy profile of the C_p distribution is highly exact and realistic. However it may be reasonable to suppose that some physical explanation is possible for the occurrence of the complicated wavy profile of C_p appearing most distinctly in the lower supersonic span-station. Lighthill (1950, 1953) showed that a finite compression wave incident on a sonic flow plane is reflected as a pressure ridge, that is, as a rapid compression followed by a rapid expansion. If the incident pressure wave has a singularity of a finite discontinuity, then the reflected one has a logarithmic singularity. Although Lighthill's study is concerned with a two-dimensional flow régime, it would be possible to consider that reflexion and interference of disturbances in the sonic flow plane should induce also in the present three-dimensional flow complicated pressure patterns especially near sonic span-stations.

Lift and downwash. Figure 9 shows the spanwise variation of the local lift coefficient C_l for the four different shear flows denoted by $M_1 \equiv M_{-\infty}(\lambda) = M_0 e^{a}$. In general C_l is lower at higher Mach numbers. The reason is obvious for the subsonic régime; it is due to the downwash induced by the trailing vorticity. The upwash distributions in the Trefftz plane are shown in figure 11. On the other hand, since no disturbance can propagate upstream in the supersonic region, no downwash seems to be induced at supersonic span. However, this conjecture is not correct in the case of a transonic shear flow, since in this case a disturbance can propagate upstream by way of the subsonic region. The disturbance upstream of the aerofoil part in the subsonic region, passing into the supersonic region across the sonic plane, reaches the aerofoil part in the supersonic region by propagating downstream in a local Mach conoid. Therefore, as long as the basic flow includes the subsonic flow region, the downwash effect, though smaller, is considered to exist at the supersonic span-station too.

In the case of a pure supersonic shear flow no disturbance can exist upstream of the aerofoil. In this case, however, the absolute lift coefficient C_l^*, or in other words the lift force itself, decreases as $M_{-\infty}$ increases (figure 10). Therefore the local lift coefficient C_l defined by (38) shows a spanwise variation similar to that for subsonic or transonic shear flow. Since the lift force variation along the span for the pure supersonic shear flow of $M_{-\infty\,\max} = 2{\cdot}718$ is opposite to those for the other shear flows, the patterns of the upwash $[w_\infty/U]_{z=0}$ (figure 11) as well as the cross-flow component $[v_\infty/U]_{z=+0}$ (figure 12) show also opposite spanwise variations to those for the other cases.

It is interesting that the trailing vorticity which is proportional to $[v_\infty/U]_{z=+0}$ is found to be stationary near the sonic station. Accordingly the spanwise gradient of C_l or C_l^* seems to be small at the sonic span-station as seen from figure 9 or 10.

In order to see how the disturbance reaches upstream of the aerofoil part in the supersonic flow region, the z-component of the disturbance velocity at the station upstream of the leading edge by 5 % chord length ($x = -0{\cdot}55$, $z = 0$) is calculated (figure 13). The large value in the subsonic region is due to the contribution of the leading edge singularity. It is seen that the upstream disturbance in the supersonic part decreases with increase of the supersonic flow region. From a theoretical standpoint no disturbance exists upstream of the aerofoil in the case of an entirely supersonic shear flow, and it is confirmed numerically within the limit of the computational error.

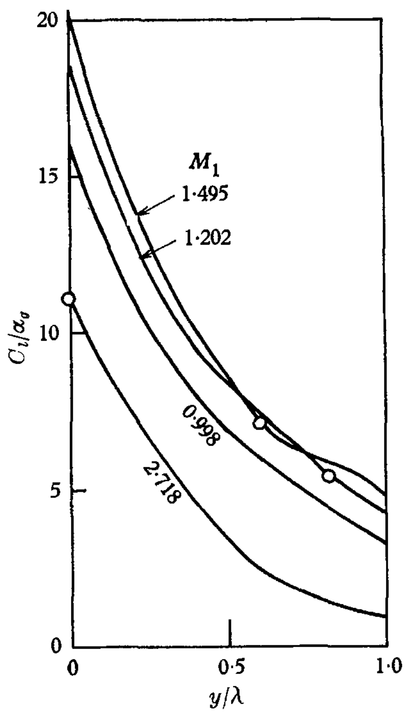

FIGURE 9

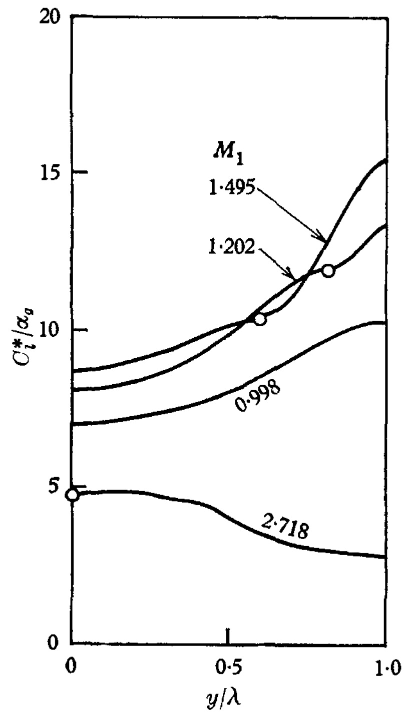

FIGURE 10

FIGURE 9. Spanwise distribution of the local lift coefficient for a flat plate of $\lambda = 2{\cdot}5$ in shear flows of $a = 1{\cdot}0$. The open circle ○ denotes the sonic span-station.

FIGURE 10. Spanwise distribution of the absolute lift coefficient defined by (41) for a flat plate of $\lambda = 2{\cdot}5$ in shear flows of $a = 1{\cdot}0$. The open circle ○ denotes the sonic span-station.

Finally, the mean local lift coefficient defined by

$$\bar{C}_l \equiv \frac{1}{\lambda}\int_0^\lambda C_l\, dy \tag{42}$$

is shown in figure 14. It is found that $\bar{C}_l$ becomes maximum at the harmonic mean Mach number $\bar{M}^*_{-\infty}$ of about 0·8 at least for this type of shear flow ($a = 1{\cdot}0$).

9. Conclusion

An extensive linear theory is developed for a thin aerofoil in a transonic shear flow with spanwisely non-uniform Mach number. By solving the basic differential equation of mixed type a generalized expression for disturbance pressure due to a sheet of pressure dipoles is derived in a Fourier integral form which holds for not only transonic but also pure supersonic or pure subsonic shear flows.

A set of integral equations is derived to determine the pressure distribution on the aerofoil surface. A method of numerical solution is shown, where the disturbance pressure at the trailing edge is assumed to be finite for all the flow régimes.

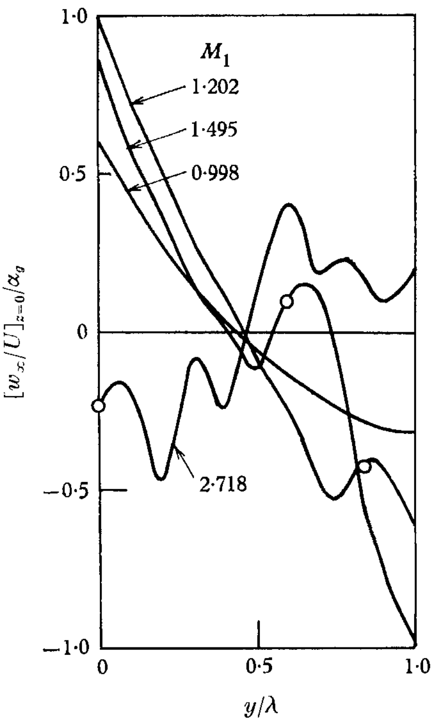

FIGURE 11

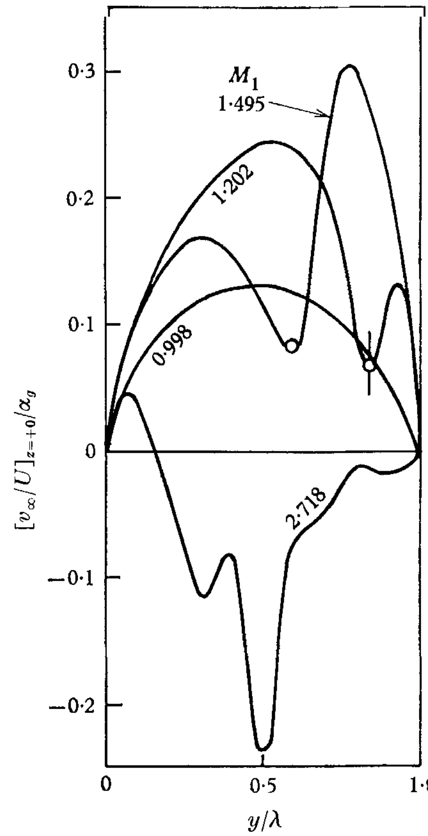

FIGURE 12

FIGURE 11. Spanwise distribution of the z-component of the induced velocity on the wake surface far downstream for a flat plate of $\lambda = 2{\cdot}5$ in shear flows of $a = 1{\cdot}0$. The open circle ○ denotes the sonic span-station.

FIGURE 12. Spanwise distribution of the y-component of the induced velocity on the wake surface far downstream for a flat plate of $\lambda = 2{\cdot}5$ in shear flows of $a = 1{\cdot}0$. The open circle ○ denotes the sonic span-station.

The numerical results indicate that the three-dimensional effect of the non-uniform Mach number on the surface pressure distribution is most violent at lower supersonic span-stations, where the chordwise pressure profiles show complicated forms with mixed supersonic and subsonic characters, and further no such great lift force arises as would be expected from the linearized uniform flow theory. On the other hand over almost the whole subsonic span-station and higher supersonic span-stations the surface pressure distributions are similar in character to those in uniform subsonic and supersonic flows respectively.

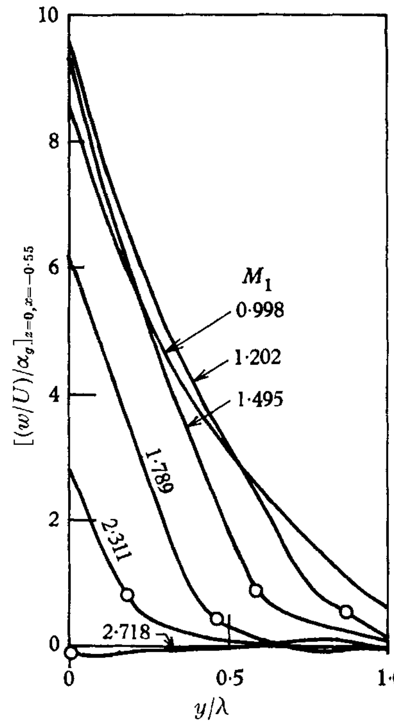

FIGURE 13. Spanwise distribution of the z-component of the induced velocity upstream of the leading edge ($z = 0$, $x = -0{\cdot}55$) for a flat plate of $\lambda = 2{\cdot}5$ in shear flows of $a = 1{\cdot}0$. The open circle ○ denotes the sonic span-station.

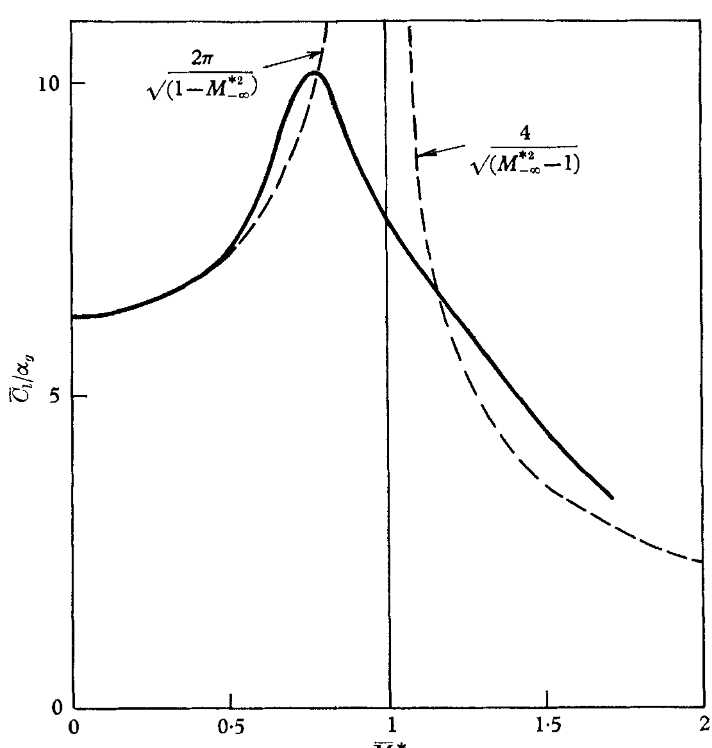

FIGURE 14. Variation of the mean local lift coefficient defined by (42) with the harmonic mean Mach number for a flat plate of $\lambda = 2{\cdot}5$ in shear flows of $a = 1{\cdot}0$.

The author is indebted to Prof. T. Asanuma and Associate Prof. Y. Tanida of the Institute of Space and Aeronautical Science, University of Tokyo, as well as to Profs. T. Okazaki and J. Kondo of the Department of Aeronautics, University of Tokyo, for their invaluable advice and encouragement.

Appendix A. Proof of (18)

It is evident that the expression (18) satisfies the boundary condition (3), since $Y_n(y;\alpha)$ is the solution of (8) and (9). The discontinuity of pressure across the lifting-surface is confirmed by using (16) as follows:

$$
\begin{aligned}
[p]_{z=\pm 0} &= \mp \int_{-\frac{1}{2}}^{\frac{1}{2}} d\xi \int_0^\infty \cos\{\alpha(x-\xi)\} \sum_{n=0}^{\infty} F_n(\xi;\alpha)\, Y_n(y;\alpha)\, d\alpha \\
&= \mp \frac{1}{2\pi}\int_{-\frac{1}{2}}^{\frac{1}{2}} \Delta p_s(\xi,y) \int_0^\infty \cos\{\alpha(x-\xi)\}\, d\alpha\, d\xi \\
&= \mp \frac{1}{2}\int_{-\frac{1}{2}}^{\frac{1}{2}} \Delta p_s(\xi,y)\,\delta(x-\xi)\, d\xi \\
&= \begin{cases} \mp \frac{1}{2}\Delta p_s(x,y) & (|x| \leqslant \frac{1}{2}), \\ 0 & (|x| > \frac{1}{2}), \end{cases}
\end{aligned} \tag{A 1}
$$

where $\delta(x-\xi)$ denotes the delta function of Dirac.

Now, it is necessary to confirm that (18) satisfies the boundary condition at infinity given by (5) and (6). Let us introduce $FY_n(x,y;\alpha)$ defined by

$$FY_n(x,y;\alpha) = F_n(x;\alpha)\, Y_n(y;\alpha) - F_n(x;\infty)\, Y_n(y;\infty). \tag{A 2}$$

From the relations (11), (12) and (17), it follows that

$$FY_n(x,y;\alpha) = O(\alpha^{-2}) \quad \text{as} \quad \alpha \to \infty. \tag{A 3}$$

Let the infinite series in the integrand of (18) be approximated by the truncated series with the first N terms retained. Then p can be expressed in terms of the following three portions:

$$p = p^{(1)} + p^{(2)} + p^{(3)}, \tag{A 4}$$

where

$$
\begin{aligned}
p^{(1)} &= -\operatorname{sgn} z \int_{-\frac{1}{2}}^{\frac{1}{2}} d\xi \int_0^\infty \sum_{n=0}^{N-1} \mathscr{R}[\exp(i\alpha(x-\xi) - \beta_n(\alpha)|z|)]\, FY_n(\xi,y;\alpha)\, d\alpha \\
&= -\operatorname{sgn} z \int_{-\frac{1}{2}}^{\frac{1}{2}} d\xi \sum_{n=0}^{N-1} \mathscr{R}\left[\int_0^\infty \exp(i\alpha(x-\xi) - \beta_n(\alpha)|z|)\, FY_n(\xi,y;\alpha)\right] d\alpha,
\end{aligned} \tag{A5}
$$

$$
\begin{aligned}
p^{(2)} &= -\operatorname{sgn} z \int_{-\frac{1}{2}}^{\frac{1}{2}} d\xi \int_0^\infty \sum_{n=N'}^{N-1} \mathscr{R}[\exp(i\alpha(x-\xi) - \beta_n(\alpha)|z|)]\, F_n(\xi;\infty)\, Y_n(y;\infty)\, d\alpha \\
&= -\operatorname{sgn} z \int_{-\frac{1}{2}}^{\frac{1}{2}} \sum_{n=N'}^{N-1} F_n(\xi;\infty)\, Y_n(y;\infty)\, d\xi \int_0^\infty \cos\{\alpha(x-\xi)\} \exp(-\beta_n(\alpha)|z|)\, d\alpha,
\end{aligned} \tag{A 6}
$$

$$
\begin{aligned}
p^{(3)} &= -\operatorname{sgn} z \int_{-\frac{1}{2}}^{\frac{1}{2}} d\xi \int_0^\infty \sum_{n=0}^{N'-1} \mathscr{R}[\exp(i\alpha(x-\xi) - \beta_n(\alpha)|z|)]\, F_n(\xi;\infty)\, Y_n(y;\infty)\, d\alpha \\
&= -\operatorname{sgn} z \int_{-\frac{1}{2}}^{\frac{1}{2}} d\xi \sum_{n=0}^{N'-1} F_n(\xi;\infty)\, Y_n(y;\infty) \int_0^\infty \mathscr{R}[\exp(i\alpha(x-\xi) - \beta_n(\alpha)|z|)]\, d\alpha.
\end{aligned} \tag{A 7}
$$

Taking into account (12), (13) and (A 3), we find that

$$\int_0^\infty |\exp(-\beta_n(\alpha)|z|)\, FY_n(x,y;\alpha)|\, d\alpha < \infty \quad \text{for all } n \tag{A 8}$$

as well as
$$\int_0^\infty \exp(-\beta_n(\alpha)|z|)\, d\alpha < \infty \quad \text{for} \quad N' \leqslant n \leqslant N-1. \tag{A 9}$$

Then from the Riemann–Lebesgue theorem

$$p^{(1)},\ p^{(2)} \to 0 \quad \text{as} \quad x \to \pm\infty. \tag{A 10}$$

Finally, we must evaluate the following integral in $p^{(3)}$:

$$P_n \equiv -\operatorname{sgn} z \int_0^\infty \mathscr{R}[\exp(i\alpha(x-\xi) - \beta_n(\alpha)|z|)]\, d\alpha. \tag{A 11}$$

Introduce $\Omega_n(\alpha)$ such that

$$\beta_n(\alpha) = \Omega_n(\alpha)(\alpha_n^2 - \alpha^2)^{\frac{1}{2}}. \tag{A 12}$$

Then from (12), (13) and (19) it follows that

$$\left.\begin{aligned} &0 < \Omega_n(\alpha) < \infty \quad \text{for} \quad 0 < \alpha < \infty \\ \text{and} \quad &\Omega_n(\alpha) = |q_n| + O(\alpha^{-2}) \quad (\alpha \to \infty). \end{aligned}\right\} \tag{A 13}$$

Here the argument of $(\alpha_n^2 - \alpha^2)^{\frac{1}{2}}$ for $\alpha_n < \alpha$ is chosen as $\frac{1}{2}\pi$. Then we can evaluate P_n by dividing it into the following three parts:

$$P_n = P_n^{(1)} - \operatorname{sgn} z (P_n^{(2)} + P_n^{(3)}), \tag{A 14}$$

where
$$P_n^{(1)} \equiv -\operatorname{sgn} z \int_0^\infty \mathscr{R}[\exp(i\alpha x - |q_n z| \sqrt{(\alpha_n - \alpha^2)})]\, d\alpha, \tag{A 15}$$

$$P_n^{(2)} \equiv \int_0^{\alpha_n} \cos\alpha x [\exp(-\Omega_n(\alpha)\sqrt{(\alpha_n^2 - \alpha^2)}|z|) - \exp(-|q_n z| \sqrt{(\alpha_n^2 - \alpha^2)})]\, d\alpha, \tag{A 16}$$

$$P_n^{(3)} \equiv \int_{\alpha_n}^\infty [\cos\{\alpha x - \Omega_n(\alpha)\sqrt{(\alpha^2 - \alpha_n^2)}|z|\} - \cos\{\alpha x - |q_n z| \sqrt{(\alpha^2 - \alpha_n^2)}\}]\, d\alpha. \tag{A 17}$$

Since the integrand in (A 16) is bounded in the finite interval $0 < \alpha < \alpha_n$, the Riemann–Lebesgue theorem leads us to

$$\lim_{x \to \pm\infty} P_n^{(2)} = 0. \tag{A 18}$$

As to $P_n^{(3)}$, it can be written as

$$\begin{aligned} P_n^{(3)} = &-2\int_{\alpha_n}^\infty \sin\{\alpha(x - |q_n z|)\} \cos\left[\alpha|z| \left(\frac{\Omega_n(\alpha) + |q_n|}{2} \sqrt{\left(1 - \frac{\alpha_n^2}{\alpha^2}\right)} - |q_n|\right)\right] \\ &\times \sin\left[\alpha|z| \frac{|q_n| - \Omega_n(\alpha)}{2} \sqrt{\left(1 - \frac{\alpha_n^2}{\alpha^2}\right)}\right] d\alpha \\ &+ 2\int_{\alpha_n}^\infty \cos\{\alpha(x - |q_n z|)\} \sin\left[\alpha|z| \left(\frac{\Omega_n(\alpha) + |q_n|}{2} \sqrt{\left(1 - \frac{\alpha_n^2}{\alpha^2}\right)} - |q_n|\right)\right] \\ &\times \sin\left[\alpha|z| \frac{|q_n| - \Omega_n(\alpha)}{2} \sqrt{\left(1 - \frac{\alpha_n^2}{\alpha^2}\right)}\right] d\alpha. \end{aligned} \tag{A 19}$$

From (A 13), it follows that for $\alpha \to \infty$

$$\left.\begin{aligned} \cos\left[\alpha|z|\left(\frac{\Omega_n(\alpha)+|q_n|}{2}\sqrt{\left(1-\frac{\alpha_n^2}{\alpha^2}\right)}-|q_n|\right)\right] &= 1+O\left(\frac{z^2}{\alpha^2}\right),\\ \sin\left[\alpha|z|\left(\frac{\Omega_n(\alpha)+|q_n|}{2}\sqrt{\left(1-\frac{\alpha_n^2}{\alpha^2}\right)}-|q_n|\right)\right] &= O\left(\frac{|z|}{\alpha}\right),\\ \sin\left[\alpha|z|\,\frac{|q_n|-\Omega_n(\alpha)}{2}\sqrt{\left(1-\frac{\alpha_n}{\alpha^2}\right)}\right] &= O\left(\frac{|z|}{\alpha}\right). \end{aligned}\right\} \tag{A 20}$$

Then applying Fourier's single integral-theorem to the first integral of (A 19) and the Riemann–Lebesgue theorem to the second integral, we find that

$$P_n^{(3)} \to 0 \quad \text{as} \quad x-|q_n z| \to \pm\infty. \tag{A 21}$$

To evaluate $P_n^{(1)}$, consider the following formula (Morse & Feshbach 1953):

$$I \equiv \int_{-\infty}^{\infty} \frac{\exp(i\alpha x - i|q_n z|\sqrt{(\alpha^2-\alpha_n^2)})}{\sqrt{(\alpha^2-\alpha_n^2)}}\,d\alpha = \left\{\begin{array}{ll} 0 & (x<|q_n z|),\\ -(2\pi/i)\,J_0(\alpha_n\sqrt{(x^2-q_n^2z^2)}) & (x>|q_n z|), \end{array}\right\} \tag{A 22}$$

where

$$\sqrt{(\alpha^2-\alpha_n^2)} = \begin{cases} \alpha\sqrt{\{1-(\alpha_n^2/\alpha^2)\}} & (|\alpha|>\alpha_n),\\ -i\sqrt{(\alpha_n^2-\alpha^2)} & (|\alpha|<\alpha_n), \end{cases}$$

and J_0 is the Bessel function of the first kind of order zero. The integral I can be rewritten as

$$I = 2i\left[\int_{\alpha_n}^{\infty} \frac{\sin\{\alpha x-|q_n z|\sqrt{(\alpha^2-\alpha_n^2)}\}}{\sqrt{(\alpha^2-\alpha_n^2)}}\,d\alpha + \int_0^{\alpha_n} \frac{\cos\alpha x\exp(-|q_n z|\sqrt{(\alpha_n^2-\alpha^2)})}{\sqrt{(\alpha_n^2-\alpha^2)}}\,d\alpha\right]. \tag{A 22a}$$

Therefore

$$\frac{\partial I}{\partial z} = -2i\,\mathrm{sgn}\,z\,|q_n|\left[\int_{\alpha_n}^{\infty}\cos\{\alpha x-|q_n z|\sqrt{(\alpha^2-\alpha_n^2)}\}\,d\alpha + \int_0^{\alpha_n}\cos\alpha x\exp(-|q_n z|\sqrt{(\alpha_n^2-\alpha^2)})\,d\alpha\right]. \tag{A 23}$$

Then it follows from (A 15) and (A 23) that

$$P_n^{(1)} = \frac{1}{2i|q_n|}\frac{\partial I}{\partial z}. \tag{A 24}$$

Therefore from (A 22)

$$P_n^{(1)} = \left\{\begin{array}{ll} 0 & (x<|q_n z|),\\ \dfrac{\pi}{|q_n|}\dfrac{\partial}{\partial z}J_0(\alpha_n\sqrt{(x^2-q_n^2z^2)}) & (x>|q_n z|). \end{array}\right\} \tag{A 25}$$

Consequently it turns out that

$$\left.\begin{array}{lll} |p^{(3)}|<\infty & \text{for} & x>-\tfrac{1}{2},\\ p^{(3)}\to 0 & \text{as} & x\to-\infty. \end{array}\right\} \tag{A 26}$$

Appendix B. Derivation of (22)

Putting

$$I_n^{(1)} \equiv -\operatorname{sgn} z \int_0^\infty \mathscr{R}[\exp(i\alpha(x-\xi)-\beta_n(\alpha)|z|)]\, FY_n(\xi, y; \alpha)\, d\alpha, \tag{B 1}$$

$$I_n^{(2)} \equiv -\operatorname{sgn} z \int_0^\infty \mathscr{R}[\exp(i\alpha(x-\xi)-\beta_n(\alpha)|z|)]\, d\alpha, \tag{B 2}$$

we can rewrite (20) as

$$\left[\frac{w}{U}\right]_{z=0} = -\frac{1}{\kappa p_{-\infty} M_{-\infty}^2} \int_{-\frac{1}{2}}^{\frac{1}{2}} \sum_{n=0}^{N-1} \left[\int_{-\infty}^{x} \frac{\partial I_n^{(1)}}{\partial z}\, dx + F_n(\xi;\infty)\, Y_n(y;\infty) \int_{-\infty}^{x} \frac{\partial I_n^{(2)}}{\partial z}\, dx\right]_{z=0} d\xi. \tag{B 3}$$

Since the terms for $n > N'$ in (23) can be derived in the same way as shown in S, derivation of the terms for $0 \leqslant n \leqslant N'-1$ only will be demonstrated here.

For $0 \leqslant n \leqslant N'-1$

$$\left[\int_{-\infty}^{x} \frac{\partial I_n^{(1)}}{\partial z}\, dx\right]_{z=0} = \left[\int_0^{\alpha_n} \sin\{\alpha(x-\xi)\} \frac{\beta_n(\alpha)}{\alpha} FY_n(\xi, y; \alpha)\, d\alpha\right]_{x=-\infty}^{x} + \left[\int_{\alpha_n}^{\infty} \cos\{\alpha(x-\xi)\} \frac{\beta_n(\alpha)}{\alpha} FY_n(\xi, y; \alpha)\, d\alpha\right]_{x=-\infty}^{x}, \tag{B 4}$$

which, if (12) and (A 3) are considered, becomes

$$\left[\int_{-\infty}^{x} \frac{\partial I_n^{(1)}}{\partial z}\, dx\right]_{z=0} = \tfrac{1}{2}\pi \beta_n^{(0)} FY_n(\xi, y; 0) + \int_0^{\alpha_n} \sin\{\alpha(x-\xi)\} \frac{\beta_n(\alpha)}{\alpha} FY_n(\xi, y; \alpha)\, d\alpha + \int_{\alpha_n}^{\infty} \cos\{\alpha(x-\xi)\} \frac{\beta_n(\alpha)}{\alpha} FY_n(\xi, y; \alpha)\, d\alpha. \tag{B 4a}$$

On the other hand also for $0 \leqslant n \leqslant N'-1$ we have

$$\left[\int_{-\infty}^{x} \frac{\partial I_n^{(2)}}{\partial z}\, dx\right]_{z=0} = \left[\int_0^{\alpha_n} \sin\{\alpha(x-\xi)\} \frac{\beta_n(\alpha)}{\alpha}\, d\alpha\right]_{x=-\infty}^{x} + \left[\int_{\alpha_n}^{\infty} \cos\{\alpha(x-\xi)\} \frac{\beta_n(\alpha)}{\alpha}\, d\alpha\right]_{x=-\infty}^{x}. \tag{B 5}$$

The first definite integral on the right-hand side of (B 5) is rewritten as

$$\left[\int_0^{\alpha_n} \sin\{\alpha(x-\xi)\} \frac{\beta_n(\alpha)}{\alpha}\, d\alpha\right]_{x=-\infty}^{x} = \tfrac{1}{2}\pi \beta_n^{(0)} + \int_0^{\alpha_n} \sin\{\alpha(x-\xi)\} \frac{\beta_n(\alpha)}{\alpha}\, d\alpha, \tag{B 6}$$

while the second infinite integral, if (12) is considered, becomes

$$\left[\int_{\alpha_n}^{\infty} \cos\{\alpha(x-\xi)\}\frac{\beta_n(\alpha)}{\alpha}d\alpha\right]_{x=-\infty}^{x} = \left[\int_{\alpha_n}^{\infty} \cos\{\alpha(x-\xi)\}\left\{\frac{\beta_n(\alpha)}{\alpha}-|q_n|\right\}d\alpha\right]_{x=-\infty}^{x}$$
$$+|q_n|\left[\int_0^{\infty}\cos\{\alpha(x-\xi)\}d\alpha - \int_0^{\alpha_n}\cos\{\alpha(x-\xi)\}d\alpha\right]_{x=-\infty}^{x}$$
$$= \int_{\alpha_n}^{\infty}\cos\{\alpha(x-\xi)\}\left\{\frac{\beta_n(\alpha)}{\alpha}-|q_n|\right\}d\alpha + |q_n|\left[\pi\delta(x-\xi)-\frac{\sin\{\alpha_n(x-\xi)\}}{x-\xi}\right]. \qquad \text{(B 7)}$$

Using the above results and taking (11) and (21) into account, we can finally get the expression (22).

Appendix C. A brief comment on the thickness effect

The effect of thickness on the pressure field corresponds to that of the pressure dipoles which have axes parallel to the basic flow. The disturbance pressure p_τ due to such dipoles distributed on the aerofoil surface ($z = 0$, $-\frac{1}{2} < x < \frac{1}{2}$) will be represented by

$$p_\tau = -\int_{-\frac{1}{2}}^{\frac{1}{2}} d\xi \int_0^{\infty} \sum_{n=0}^{\infty} \frac{\partial}{\partial x}\mathscr{R}\left[\exp(i\alpha(x-\xi)-\beta_n(\alpha)|z|)\frac{1}{\beta_n(\alpha)}\right] G_n(\xi;\alpha)\, Y_n(y;\alpha)\, d\alpha. \qquad \text{(C 1)}$$

Then the z-component of the velocity induced on the plane $z = 0$ is written as

$$\left[\frac{w}{U}\right]_{z=\pm 0} = -\frac{1}{\kappa p_{-\infty} M_{-\infty}^2}\left[\int_{-\infty}^{x}\frac{\partial p}{\partial z}dx\right]_{z=\pm 0}$$
$$= \pm\frac{1}{\kappa p_{-\infty} M_{-\infty}^2}\int_{-\frac{1}{2}}^{\frac{1}{2}} d\xi\int_0^{\infty}\cos\{\alpha(x-\xi)\}\sum_{n=0}^{\infty} G_n(\xi;\alpha)\, Y_n(y;\alpha)\, d\alpha. \qquad \text{(C 2)}$$

Therefore the $G_n(x;\alpha)$ are associated with the aerofoil thickness distribution by the following relation:

$$\left.\begin{aligned} g(x,y) &= \frac{\pi}{\kappa p_{-\infty} M_{-\infty}^2}\sum_{n=0}^{\infty} G_n(x;\alpha)\, Y_n(y;\alpha), \\ \text{or}\qquad G_n(x;\alpha) &= \frac{\kappa p_{-\infty}}{\pi}\frac{1}{\lambda}\int_0^{\lambda} g(x,y)\, Y_n(y;\alpha)\, dy, \end{aligned}\right\} \qquad \text{(C 3)}$$

where $g(x,y)$ denotes the contribution of thickness to the slope of the aerofoil surface.

The results of the more detailed studies on the thickness effect are to be reported in the future.

REFERENCES

LIEBLEIN, S., LEWIS, G. W. & SANDERCOCK, D. M. 1952 *NACA RM* E52A24.

LIGHTHILL, M. J. 1950 *Quart. J. Mech. Appl. Math.* **3**, 303.

LIGHTHILL, M. J. 1953 *Proc. Roy. Soc.* A **217**, 478.

McCUNE, J. E. 1958 *J. Aeron. Space Sci.* **25**, 616.

MORSE, P. M. & FESHBACH, H. 1953 *Methods of Theoretical Physics*, I. New York: McGraw-Hill.

NAMBA, M. 1969 *J. Fluid Mech.* **36**, 735.

NAMBA, M. & ASANUMA, T. 1965 *Trans. Japan Soc. Mech. Engrs* **31**, 1236 (in Japanese); *Bull. Inst. Space Aeron. Sci.* Univ. Tokyo, **1**, 164 (in Japanese).

NAMBA, M. & ASANUMA, T. 1967 *Bull. Japan Soc. Mech. Engrs* **10**, 920; *Rep. of Inst. Space Aeron. Sci.* Univ. Tokyo, **32**, 133.